Articles

Structure and Dynamics of Half-Sandwich Ruthenium(IV) Alkynyl Hydrido Complexes[†]

Halikhedkar Aneetha, Manuel Jiménez-Tenorio, M. Carmen Puerta, and
Pedro Valerga*

*Departamento de Ciencia de Materiales e Ingeniería Metalúrgica y Química Inorgánica,
Facultad de Ciencias, Universidad de Cádiz, 11510 Puerto Real, Cádiz, Spain*

Kurt Mereiter

*Institute of Chemical Technologies and Analytics, Vienna University of Technology,
Getreidemarkt 9, A-1060 Vienna, Austria*

The coordinatively unsaturated complex [Cp*Ru(PMe^{i}Pr$_2$)$_2$][BAr′$_4$] (**1**; BAr′$_4$ = B{3,5-C$_6$H$_3$-(CF$_3$)$_2$}$_4$) reacts with 1-alkynes in diethyl ether at 0 °C, furnishing the Ru^{IV} alkynyl hydrido derivatives [Cp*RuH(C≡CR)(PMe^{i}Pr$_2$)$_2$][BAr′$_4$]. In an analogous fashion, the reaction of **1** with 1-alkyn-3-ols in diethyl ether at 0 °C leads to the 3-hydroxyalkynyl hydrido complexes [Cp*RuH(C≡CC(OH)RR′)(PMe^{i}Pr$_2$)$_2$][BAr′$_4$]. The complexes [Cp*RuH(C≡CCOOMe)(PMe^{i}Pr$_2$)$_2$][BAr′$_4$] and [Cp*RuH(C≡CC(OH)Ph$_2$)(PMe^{i}Pr$_2$)$_2$][BAr′$_4$]·Et$_2$O have been structurally characterized, and their crystal structures show a transoid disposition of the hydride and alkynyl ligands. These compounds are stereochemically nonrigid and undergo a rapid equilibrium between possible stereoisomers in solution, which has been studied by variable-temperature NMR spectroscopy and computer simulation. The dynamic NMR study for these processes indicates energy barriers of ca. 11 kcal mol^{-1}, and moreover the differences in energy for the possible stereoisomers are very small (ca. 1 kcal mol^{-1}). The alkynyl hydrido complexes rearrange to their more stable vinylidene or hydroxyvinylidene tautomers. Spontaneous dehydration of the latter leads to either vinylvinylidene or allenylidene complexes.

Introduction

Since our initial report on the formation of metastable half-sandwich Ru^{IV} alkynyl hydrido complexes [Cp*RuH-(C≡CR)(dippe)]$^+$ (dippe = 1,2-bis(diisopropylphosphino)-ethane) as intermediates in the formation of vinylidene complexes,[1,2] we have advanced in the knowledge of the chemistry of such species. Thus, we have proven that the previously overlooked hydroxyalkynyl hydrido complexes [Cp*RuH(C≡CC(OH)RR′)(PP)]$^+$ (PP = dippe, (PEt$_3$)$_2$) are also involved in the formation of hydroxyvinylidene complexes and, therefore, in the subsequent dehydration processes leading to allenylidene, vinylvinylidene, or even hydrido enynyl derivatives.[3−6] However, the study of the structure of ruthenium alkynyl hydrido and hydroxyalkynyl hydrido complexes is made more difficult by their metastable character and the fact that, in most cases, they rearrange to their more stable vinylidene isomers in the solid state. In fact, we have carried out quantitative studies on the solid-state isomerization to vinylidene of several alkynyl hydrido complexes using IR spectroscopy as a tool.[7] Very recently, the related Os^{IV} alkynyl hydrido complexes [CpOsH(C≡CR)(P^{i}Pr$_3$)$_2$][PF$_6$] (R = Ph, Cy) as well as the hydroxyalkynyl hydrido derivatives [CpOsH(C≡CC(OH)RPh)(P^{i}Pr$_3$)$_2$][PF$_6$] (R = Me, Ph) have been reported.[8] These compounds were obtained by reaction of [CpOsCl(P^{i}Pr$_3$)$_2$] with TlPF$_6$ and the appropriate alkyne or alkynol in acetone/dichloromethane. Other Os^{IV} alkynyl hydrido complexes of the type [CpOsH(C≡

* To whom correspondence should be addressed. E-mail: pedro.valerga@uca.es.

† Dedicated to Professor G. Jeffery Leigh, as recognition of his career and outstanding contribution to inorganic and organometallic chemistry.

(1) de los Ríos, I.; Jiménez-Tenorio, M.; Puerta, M. C.; Valerga, P. *J. Chem. Soc., Chem. Commun.* **1995**, 1757.

(2) de los Ríos, I.; Jiménez-Tenorio, M.; Puerta, M. C.; Valerga, P. *J. Am. Chem. Soc.* **1997**, *119*, 6529.

(3) de los Ríos, I.; Jiménez-Tenorio, M.; Puerta, M. C.; Valerga, P. *J. Organomet. Chem.* **1997**, *549*, 221.

(4) Bustelo, E.; Jiménez-Tenorio, M.; Puerta, M. C.; Valerga, P. *Organometallics* **1999**, *18*, 950.

(5) Bustelo, E.; Jiménez-Tenorio, M.; Puerta, M. C.; Valerga, P. *Organometallics* **1999**, *18*, 4563.

(6) Bustelo, E.; Jiménez-Tenorio, M.; Puerta, M. C.; Valerga, P. *Eur. J. Inorg. Chem.* **2001**, 2391.

(7) Bustelo, E.; de los Ríos, I., Jiménez-Tenorio, M.; Puerta, M. C.; Valerga, P. *Monatsh. Chem.* **2000**, *131*, 1311.

(8) Baya, M.; Crochet, P.; Esteruelas, M. A.; Gutiérrez-Puebla, E.; López, A. M.; Modrego, J.; Oñate, E.; Vela, N. *Organometallics* **2000**, *19*, 2585.

CPh)(P^{i}Pr$_3$)(EPH$_3$)] (E = Si, Ge) are also known, although these were prepared in a different fashion, by reaction of [CpOsHCl(P^{i}Pr$_3$)(EPH$_3$)] with LiC≡CPh in THF.[9] The complex [CpOsH(C≡CPh)(P^{i}Pr$_3$)$_2$][PF$_6$] was structurally characterized by X-ray diffraction.[8] This was feasible because, at variance with the case for ruthenium compounds, osmium alkynyl hydrido derivatives do not undergo isomerization to their vinylidene tautomers in the solid state or in solution. Furthermore, they are cleanly deprotonated by strong bases, affording the neutral Os^{II} alkynyl complexes [CpOs(C≡CR)-(P^{i}Pr$_3$)$_2$], which react with HPF$_6$ in Et$_2$O to yield the corresponding vinylidene complexes [CpOs=C=CHR-(P^{i}Pr$_3$)$_2$][PF$_6$] by protonation at the β-carbon.[10] These results are consistent with the outcome of several theoretical studies performed on the acetylene to vinylidene tautomerization at a d^6 metal center.[11-16] Since the initial extended Hückel calculations carried out by Silvestre and Hoffmann,[11] most studies have concluded that the intermediacy of alkynyl hydrido complexes generated by oxidative addition of the alkyne to a d^6 metal center is too high in energy and another pathway, namely a 1,2-H shift, is preferred. This, however, does not apply to other electronic configurations, and hence, oxidative addition at a d^8 metal center is a feasible step in the formation of vinylidene complexes of Co,[17] Rh, and Ir.[18,19] Very recent DFT studies of the acetylene to vinylidene isomerization in the d^6 complexes [CpMn-(HC≡CH)(CO)$_2$][14] and [CpRu(HC≡CR)(PMe$_3$)$_2$]$^+$ (R = H, Me)[15] have successfully located and optimized the geometries of several possible intermediate complexes in its pathway to [CpMn=C=CH$_2$(CO)$_2$] or [CpRu=C=CHR(PMe$_3$)$_2$]$^+$ (R = H, Me). Among them, the alkynyl hydrides [CpMH(C≡CR)(L)$_2$]$^{n+}$, the η^2-CH agostic acetylene complexes [CpM(η^2-HC≡CR)(L)$_2$]$^{n+}$, and the η^2-vinylidene complexes [CpM(η^2-C=CH(R))(L)$_2$]$^{n+}$ (M = Mn, R = H, L = CO, n = 0; M = Ru, R = H, Me, L = PMe$_3$, n = 1) are particularly relevant.[14,15] Interestingly, the η^2-CH agostic acetylene complexes have been found to be more stable than alkynyl hydrides and in fact are considered key intermediates in the isomerization pathway to vinylidene. However, in the case of [CpRu(HC≡CH)(PMe$_3$)$_2$]$^+$, the energy barriers for the 1,2-hydrogen

shift and for the oxidative addition are almost comparable, so that the oxidative addition process might become competitive.[15] Further theoretical support for the involvement of alkynyl hydrido complexes as intermediates in the alkyne to vinylidene rearrangement has been recently found when Cp* is introduced instead of Cp in the model systems for computation.[16]

In an attempt to detect intermediates in the formation of vinylidene complexes, we had previously studied the direct interaction of 1-alkynes[2] and alkynols[5,6] at low temperature with labile complexes such as [Cp*Ru(η^2-C$_2$H$_4$)(dippe)][BPh$_4$][20] and [Cp*Ru(N$_2$)(PEt$_3$)$_2$][BPh$_4$][21] as precursors of the 16e moieties [Cp*Ru(dippe)]$^+$ and [Cp*Ru(PEt$_3$)$_2$]$^+$. Despite the fact that η^2-alkyne species were identified in some instances, the dissociation rate of the labile ligand becomes a limiting factor when the experiments are performed at low temperature, preventing the observation of direct alkyne addition products. The introduction of the noncoordinating anion [BAr′$_4$]$^-$ (BAr′$_4$ = tetrakis(3,5-bis(trifluoromethyl)phenyl)borate) has recently allowed us to isolate a series of coordinatively unsaturated cationic complexes [Cp*Ru(PP)][BAr′$_4$] (PP = dippe, PMe^{i}Pr$_2$, PEt$_3$, PPh^{i}Pr$_2$, PPh$_3$).[22] These compounds offer new possibilities for the study of the addition of 1-alkynes to a 16e metal center, without interference coming from the need of a preliminary ligand dissociation step. In this work we describe the structure and dynamic behavior of a series of half-sandwich Ru^{IV} alkynyl hydrido complexes generated by oxidative addition of 1-alkynes and alkynols to the 16e complex [Cp*Ru(PMe^{i}Pr$_2$)$_2$]-[BAr′$_4$] (**1**), as well as their subsequent transformation into vinylidene or hydroxyvinylidene complexes, and other products derived from the dehydration of the latter species.

Experimental Section

All synthetic operations were performed under a dry dinitrogen or argon atmosphere by following conventional Schlenk techniques. Tetrahydrofuran, diethyl ether, and petroleum ether (boiling point range 40–60 °C) were distilled from the appropriate drying agents. Solvents were deoxygenated by three freeze/pump/thaw cycles and stored under argon. Na-[BAr′$_4$][23] and [Cp*Ru(PMe^{i}Pr$_2$)$_2$][BAr′$_4$] (**1**)[22] were prepared according to reported procedures. IR spectra were recorded in Nujol mulls on a Perkin-Elmer FTIR Spectrum 1000 spectrophotometer. NMR spectra were taken on a Varian Unity 400 MHz or Varian Gemini 200 MHz spectrometer. Chemical shifts are given in parts per million from SiMe$_4$ (^{1}H and ^{13}C{^{1}H}) or 85% H$_3$PO$_4$ (^{31}P{^{1}H}). Diisopropylmethylphosphine and [BAr′$_4$]$^-$ protons and carbons appeared for all the compounds in the appropriate shift ranges and are not listed. The ^{1}H NMR resonance for the OH proton, when observed, appeared between 2 and 3 ppm, most times overlapping with phosphine isopropyl signals. Thermodynamic and activation parameters were obtained by a dynamic NMR line shape fitting simulation using the program DNMR3[24] incorporated into SpinWorks

(9) Baya, M.; Esteruelas, M. A.; Oñate, E. *Organometallics* **2001**, *20*, 4875.

(10) Baya, M.; Crochet, P.; Esteruelas, M. A.; López, A. M.; Modrego, J.; Oñate, E. *Organometallics* **2001**, *20*, 4291.

(11) Silvestre, J.; Hoffmann, R. *Helv. Chim. Acta* **1985**, *68*, 1461.

(12) Wakatsuki, Y.; Koga, N.; Yamazaki, H.; Morokuma, K. *J. Am. Chem. Soc.* **1994**, *116*, 8105.

(13) (a) Cadierno, V.; Gamasa, M. P.; Gimeno, J.; Pérez-Carreño, E.; García-Granda, S. *Organometallics* **1999**, *18*, 2821. (b) Cadierno, V.; Gamasa, M. P.; Gimeno, J.; González-Bernardo, C.; Pérez-Carreño, E.; García-Granda, S. *Organometallics* **2001**, *20*, 5177.

(14) De Angelis, F.; Sgamellotti, A.; Re, N. *Organometallics* **2002**, *21*, 2715.

(15) De Angelis, F.; Sgamellotti, A.; Re, N. *Organometallics* **2002**, *21*, 5944.

(16) Bustelo, E.; Carbó, J.; Lledós, A.; Mereiter, K.; Puerta, M. C.; Valerga, P. *J. Am. Chem. Soc.* **2003**, *125*, 3311.

(17) Bianchini, C.; Peruzzini, M.; Vacca, A.; Zanobini, F. *Organometallics* **1991**, *10*, 3697.

(18) Wakatsuki, Y.; Koga, N.; Werner, H.; Morokuma, K. *J. Am. Chem. Soc.* **1997**, *119*, 360.

(19) Wolf, J.; Werner, H.; Serhadli, O.; Ziegler, M. L. *Angew. Chem., Int. Ed. Engl.* **1983**, *22*, 414. Werner, H.; Höhn, A. *J. Organomet. Chem.* **1984**, *272*, 105. García-Alonso, F. J.; Höhn, A.; Wolf, J.; Otto, H.; Werner, H. *Angew. Chem., Int. Ed. Engl.* **1985**, *24*, 406. Dziallas, M.; Werner, H. *J. Chem. Soc., Chem. Commun.* **1987**, 852. Rappert, T.; Nürnberg, O.; Mahr, N.; Wolf, J.; Werner, H. *Organometallics* **1992**, *11*, 4156.

(20) de los Ríos, I.; Jiménez-Tenorio, M.; Padilla, J.; Puerta, M. C.; Valerga, P. *Organometallics* **1996**, *15*, 4565.

(21) Jiménez-Tenorio, M.; Puerta, M. C.; Valerga, P. *J. Organomet. Chem.* **2000**, *609*, 161.

(22) (a) Jiménez-Tenorio, M.; Puerta, M. C.; Mereiter, K.; Valerga, P. *J. Am. Chem. Soc.* **2000**, *122*, 11230. (b) Aneetha, H.; Jiménez-Tenorio, M.; Puerta, M. C.; Valerga, P.; Sapunov, V. N.; Schmid, R.; Kirchner, K.; Mereiter, K. *Organometallics* **2002**, *21*, 5334.

(23) Brookhart, M.; Grant, B.; Volpe, A. F., Jr. *Organometallics* **1992**, *11*, 3920.

Table 1. Summary of Crystallographic Data for Compounds 2a, 2i, and 3c

	2a	**2i·Et₂O**	**3c**
formula	$C_{60}H_{65}BF_{24}O_2P_2Ru$	$C_{75}H_{83}BF_{24}O_2P_2Ru$	$C_{61}H_{71}BF_{24}P_2RuSi$
fw	1447.94	1646.23	1462.09
T (K)	297(2)	223(2)	297(2)
cryst size (mm)	$0.80 \times 0.60 \times 0.32$	$0.72 \times 0.24 \times 0.22$	$0.76 \times 0.64 \times 0.58$
cryst syst	monoclinic	triclinic	triclinic
space group	$P2_1/c$ (No. 14)	$P\bar{1}$ (No. 2)	$P\bar{1}$ (No. 2)
cell params			
a (Å)	18.667(4)	12.986(3)	14.695(3)
b (Å)	19.062(5)	14.483(3)	14.764(3)
c (Å)	18.852(4)	22.235(5)	17.085(3)
α (deg)		71.25(1)	103.21(1)
β (deg)	99.55(2)	79.88(1)	107.61(1)
γ (deg)		89.36(1)	93.00(1)
V (Å³)	6615(3)	3894(1)	3410(1)
Z	4	2	2
ρ_{calc} (g cm⁻³)	1.454	1.404	1.424
μ(Mo Kα) (cm⁻¹)	3.93	3.43	3.96
F(000)	2944	1688	1492
max, min transmissn factors	1.00, 0.78	1.00, 0.93	1.00, 0.93
θ range for data collecn (deg)	1.78−25.00	1.59−25.00	1.29−30.00
no. of rflns collected	66 842	40 655	48 863
no. of unique rflns	11 583 (R_{int} = 0.045)	13 645 (R_{int} = 0.028)	19 261 (R_{int} = 0.021)
no. of obsd rflns ($I > 2\sigma_I$)	8980	11 298	15 697
no. of params	889	1011	812
final R1, wR2 values ($I > 2\sigma_I$)	0.0497, 0.1231	0.0381, 0.0941	0.0618, 0.1729
final R1, wR2 values (all data)	0.0691, 0.1410	0.0501, 0.1025	0.0749, 0.1915
residual electron density peaks (e Å⁻³)	+0.61, −0.76	+0.46, −0.39	+1.60, −1.27

Table 2. Selected ¹H and ³¹P{¹H} NMR Data for Alkynyl Hydrido Complexes 2a−j

	R, R′	³¹P{¹H} NMR[a] δ	³¹P{¹H} NMR at 183 K		¹H NMR[b]				¹H NMR at 183 K	
			δ	²J_{PP}	Ru−H	²J_{HP}	C₅(CH_3)₅	R	R′	Ru−H	²J_{HP}
2a	COOMe	43.1 s	43.5 s (A, 69%)		−8.29 t	31.9	1.86	3.64		−8.71 t (A, 69%)	31.8
			43.0 br (B, 31%)							−8.30 t (B, 31%)	27.5
2b	Ph	42.7 s	42.6 s (A, 69%)		−8.56 t	31.9	1.84	6.98, 7.14,		−8.93 t (A, 69%)	30.3
			43.3 d, 43.6 d (B, 31%)	15.2				7.25		−8.52 t (B, 31%)	32.6
2c	SiMe₃	42.2 s	41.9 s (A, 68%)		−8.64 t	31.9	1.79	0.06		−9.01 t (A, 68%)	30.3
			42.4 d, 43.6 d (B, 32%)	15.4						−8.63 t (B, 32%)	32.8
2d	H, H	42.6 s	42.5 s (A, 75%)		−8.70 t	32.1	1.79	4.36		−9.03 t (A, 75%)	31.3
			42.9 d, 43.2 d (B, 25%)	14.5						−8.62 t (B, 25%)	33.5
2e	CH₃, H	42.4 s	42.1 d, 42.3 d (A, 64%)	14.5	−8.61 t	32.0	1.82	1.39 d	4.62	−9.04 t (A, 64%)	32.8
			42.5 br, 42.9 br (B₁, 18%)					(³J_{HH} = 6.4)		−8.65 t	29.7
			42.7 br, 43.4 br (B₂, 18%)							(B₁ + B₂, 36%)	
2f	Ph, H	42.6 s	42.2 d, 42.6 d (A, 64%)	14.8	−8.61 t	31.9	1.78	7.28, 7.36,	5.56	−9.05 t (A, 64%)	32.3
			42.8 d, 43.7 d (B₁, 18%)	13.2				7.40		−8.65 t	29.7
			43.0 d, 43.8 d (B₂, 18%)	14.3						(B₁ + B₂, 36%)	
2g	CH₃, CH₃	42.2 s	41.9 s (A, 61%)		−8.60 t	32.2	1.82	1.48		−9.04 t (A, 61%)	30.9
			42.5 d, 43.5 d (B, 39%)	14.4						−8.65 t (B, 39%)	32.6
2h	Ph, CH₃	42.6 d, 42.4 d	42.1 d, 41.7 d (A, 56%)	15.3	−8.61 t	32.5	1.78	7.25, 7.34,	1.94	−9.08 t (A, 56%)	31.4
		(12 Hz)	42.5 d, 44.1 d (B₁, 22%)	13.4				7.45		−8.68 t	33.5
			42.6 d, 44.0 d (B₂, 22%)	14.0						(B₁ + B₂, 44%)	
2i	Ph, Ph	42.8 s	41.8 s (A, 42%)		−8.58 t	32.1	1.80	7.28, 7.33,		−9.06 t (A, 42%)	30.4
			42.7 d, 44.7 d (B, 58%)	14.0				7.54		−8.68 t (B, 58%)	32.6
2j	C₅H₁₀	42.2 s	41.4 s (A₁, 29%)		−8.62 t	32.8	1.82	1.64, 1.95		−9.18 t (A₁, 29%)	30.0
			41.7 s (A₂, 29%)							−9.09 t (A₂, 29%)	29.0
			42.1 d, 43.5 d (B₁, 21%)	14.5						−8.77 t (B₁, 21%)	33.3
			42.3 d, 44.3 d (B₂, 21%)	12.5						−8.71 t (B₂, 21%)	33.3

[a] Conditions: 161.89 MHz, CD₂Cl₂, 273 K. δ in ppm, and coupling constants in Hz. [b] Conditions: 400 MHz, CD₂Cl₂, 273 K. δ in ppm, and coupling constants in Hz.

1.3.[25] Microanalysis was performed by the Serveis Científico-Tècnics, Universitat de Barcelona.

Alkynyl Hydrido Complexes [Cp*RuH(C≡CR)-(PMeⁱPr₂)₂][BAr′₄] (R = COOMe (2a), Ph (2b), SiMe₃ (2c)) and 3-Hydroxyalkynyl Hydrido Complexes [Cp*RuH{C≡CC(OH)RR′}(PMeⁱPr₂)₂][BAr′₄] (R, R′ = H, H (2d), H, CH₃ (2e), H, Ph (2f), CH₃, CH₃ (2g), CH₃, Ph (2h), Ph, Ph (2i), C₅H₁₀ (2j)). To a solution of **1** (0.272 g, 0.2 mmol) in 5 mL of CH₂Cl₂ at 0 °C was added the corresponding alkyne or hydroxyalkyne (0.2 mmol). The color immediately changed from blue to colorless or pale yellow. The reaction mixture was stirred for 10 min at 0 °C. Then, most of the solvent was removed in vacuo. Addition of petroleum ether gave an off-white crystalline solid, which was filtered, washed with petroleum ether, dried, and stored at −20 °C. Yield: 80−90% in all cases. With the exception of compound **2a**, microanalysis was not carried out because these compounds rearrange to their vinylidene isomers in the solid state. Selected NMR spectral data for these compounds are given in Tables 2 and 3. **2a**: IR ν(C≡C) 2112 (s), 2093 (w, sh) cm⁻¹, ν(RuH) 2037 (w) cm⁻¹, ν(C=O) 1677 cm⁻¹. Anal. Calcd for C₆₀H₆₅BF₂₄O₂P₂-Ru: C, 49.8; H, 4.49. Found: C, 50.0; H, 4.52. **2b**: IR ν(C≡C) 2109 cm⁻¹, ν(RuH) 2020 (w) cm⁻¹. **2c**: IR ν(C≡C) 2038 cm⁻¹, ν(RuH) not observed. **2d**: IR ν(C≡C) 2121 cm⁻¹, ν(RuH) 2025 (w) cm⁻¹, ν(OH) 3625 (w) cm⁻¹. **2e**: IR ν(C≡C) 2116 cm⁻¹, ν(RuH) 2083 (w) cm⁻¹. **2f**: IR ν(C≡C) 2111 cm⁻¹, ν(RuH) 2037 (w) cm⁻¹, ν(OH) 3608 (w) cm⁻¹. **2g**: IR ν(C≡C) 2121 cm⁻¹, ν-

(24) Kleier, D. A.; Binsch, G. *J. Magn. Reson.* **1970**, *3*, 146.
(25) Marat, K. SpinWorks 1.3; University of Manitoba, 2001.

Table 3. Selected $^{13}C\{^1H\}$ NMR Data for Alkynyl Hydrido Complexes 2a−j

	R, R′	$C_5(CH_3)_5$	$C_5(CH_3)_5$	C_α	$^2J_{CP}$	C_β	C_γ	R	R′
						$^{13}C\{^1H\}$ NMR[a]			
2a	COOMe	10.3	103.1	116.0 t	29.0	109.7		51.9, 153.1	
2b	Ph	10.3	102.1	104.0 t	28.4	109.7		126.4, 128.4,130.2	
2c	SiMe₃	10.3	102.1	127.7 t	27.3	122.6		0.35	
2d	H, H	10.3	101.9	98.0 t	28.1	113.2	53.2		
2e	CH₃, H	10.3	101.9	95.6 t	27.7	116.3	60.1	25.5	
2f	Ph, H	10.3	102.0	99.6 t	28.2	115.2	66.5	125.4, 128.0, 128.6	
2g	CH₃, CH₃	10.3	101.9	93.1 t	27.9	119.8	66.4	32.1	
2h	Ph, CH₃	10.3	102.0	96.2 t	27.4	118.8	70.0	124.3, 127.0, 128.0	32.4
2i	Ph, Ph	10.4	102.2	100.7 t	27.3	116.3	75.6	126.1, 127.4, 128.1	
2j	C₅H₁₀	10.4	101.9	87.5 t	28.1	119.9	72.2	22.4, 25.0, 40.3	

[a] Conditions: 201.2 MHz, CD₂Cl₂, 273 K. δ in ppm, and coupling constants in Hz.

Table 4. Thermodynamic and Activation Parameters for the Equilibrium between Alkynyl Hydrido Isomers (A ⇆ B), with Estimated Standard Deviations in Parentheses

	$K_{eq}^{186.5}$	ΔH (kcal mol⁻¹)	ΔS (cal K⁻¹ mol⁻¹)	ΔG^{298} (kcal mol⁻¹)	$\Delta H^‡$ (kcal mol⁻¹)	$\Delta S^‡$ (cal K⁻¹ mol⁻¹)	$\Delta G^{‡298}$ (kcal mol⁻¹)
		thermodynamic params			activation params		
2a	0.47	0.48(0.01)	1.13(0.06)	0.14(0.03)	6.6(0.1)	−14.2(0.6)	11.0(0.3)
2b	0.53	0.75(0.02)	2.74(0.08)	0.07(0.04)	6.2(0.1)	−16.0(0.6)	11.0(0.3)
2c	0.51	0.97(0.05)	3.9(0.2)	−0.2(0.1)	6.8(0.3)	−14(2)	11.0(0.9)
2d	0.34	1.70(0.08)	7.1(0.4)	−0.4(0.2)	6.9(0.5)	−14(2)	11(1)
2e	0.55	0.70(0.04)	2.6(0.2)	−0.1(0.1)	6.7(0.4)	−15(2)	11(1)
2f	0.57	0.66(0.04)	2.4(0.2)	−0.1(0.1)	6.3(0.3)	−17(2)	11.3(0.9)
2g	0.64	1.10(0.03)	5.0(0.1)	−0.39(0.06)	7.6(0.6)	−11(3)	11(1)
2h	0.79	0.70(0.02)	3.3(0.1)	−0.28(0.04)	7.4(0.4)	−11(2)	11(1)
2i	1.36	0.27(0.02)	2.0(0.1)	−0.32(0.05)	6.4(0.3)	−15(1)	10.9(0.6)
2j	0.75	1.68(0.06)	8.3(0.3)	−0.8(0.1)	7.7(0.7)	−11(3)	11(2)

Table 5. Selected ^1H and $^{31}P\{^1H\}$ NMR Data for Hydroxyvinylidene Complexes 3b−j

	R, R′	δ	$^2J_{PP'}$	Ru=C=CH	$^4J_{HP}$	$C_5(CH_3)_5$	R	R′
		$^{31}P\{^1H\}$ NMR[a]		^1H NMR[b]				
3b	Ph	35.7 s		5.40 br		1.98	7.09,7.18, 7.30	
3c	SiMe₃	35.9 s		3.39 t	3.1	1.86	0.09	
3d	H, H	37.1 s		4.34 br		1.76	4.34 br	
3e	CH₃, H	37.1 s		4.12 dt	1.6	1.75	1.34 d ($^3J_{HH}$ = 8.7)	4.77 m
3f	Ph, H	36.9 d, 37.2 d	31.7	4.39 d		1.74	7.26, 7.32, 7.37	5.61 d ($^3J_{HH}$ = 8.7)
3g	CH₃,CH₃	35.1 s		3.88 br		1.76	1.37 s	
3h	Ph, CH₃	34.9 d, 35.6 d	31.7	4.25 br		1.72	7.26,7.35, 7.37	1.69 s
3i	Ph, Ph	35.5 s		4.61 br		1.73	7.26,7.29, 7.32	
3j	C₅H₁₀	35.2 s		3.94 br		1.75	1.26, 1.45	

[a] Conditions: 161.89 MHz, CDCl₃, 273 K. δ in ppm, and coupling constants in Hz. [b] Conditions: 400 MHz, CDCl₃, 273 K. δ in ppm, and coupling constants in Hz.

(RuH) 2024 (w) cm⁻¹, ν(OH) 3615 (w) cm⁻¹. **2h**: IR ν(C≡C) 2112 cm⁻¹, ν(RuH) 2038 (w) cm⁻¹, ν(OH) 3618 (w) cm⁻¹. **2i**: IR ν(C≡C) 2110 cm⁻¹, ν(RuH) 2040 (w) cm⁻¹, ν(OH) 3608 (w) cm⁻¹. **2j**: IR ν(C≡C) 2105 cm⁻¹, ν(RuH) 2016 (w) cm⁻¹, ν(OH) 3608 (w) cm⁻¹.

Vinylidene Complexes [Cp*Ru=C=CHR(PMe^{i}Pr₂)₂]-[BAr′₄] (R = Ph (3b), SiMe₃ (3c)) and 3-Hydroxyvinylidene Complexes [Cp*Ru{=C=CHC(OH)RR′}(PMe^{i}Pr₂)₂]-[BAr′₄] (R, R′ = H, H (3d), H, CH₃ (3e), H, Ph (3f), CH₃, CH₃ (3g), CH₃, Ph (3h), Ph, Ph (3i), C₅H₁₀ (3j)). A solid sample of the corresponding alkynyl hydrido derivatives **2b−j** (0.15 g) was heated to 30 °C over a period of 3−6 h. During this time, the color of the sample changed from off-white or pale yellow to orange-red. The process can be monitored by IR spectroscopy, following the decrease in the ν(C≡C) band at ∼2100 cm⁻¹ until its disappearance. Yield: quantitative. Compound **3i** undergoes spontaneous dehydration during this process, and therefore it was always obtained mixed with the allenylidene derivative **5i**. For this reason, it was not analyzed, and its NMR characterization was carried out in solutions containing mixtures of **3i** and **5i**. Selected NMR spectral data for these compounds are given in Tables 5 and 6. **2b**: IR ν-(C≡C) 1608 cm⁻¹. Anal. Calcd for C₆₄H₆₇BF₂₄P₂Ru: C, 52.4; H, 4.57. Found: C, 52.4; H, 4.49. **3c**: IR: ν(C≡C) 1613 cm⁻¹. Anal. Calcd for C₆₁H₇₁BF₂₄P₂RuSi: C, 50.1; H, 4.86. Found:

C, 49.8; H, 4.77. **3d**: IR ν(C=C) 1643 cm⁻¹. Anal. Calcd for C₅₉H₆₅BF₂₄OP₂Ru: C, 49.9; H, 4.58. Found: C, 49.8; H, 4.62. **3e**: IR ν(C=C) 1643 cm⁻¹. Anal. Calcd for C₆₀H₆₇BF₂₄OP₂Ru: C, 50.3; H, 4.68. Found: C, 50.4; H, 4.75. **3f**: IR ν(C=C) 1641 cm⁻¹. Anal. Calcd for C₆₅H₆₉BF₂₄OP₂Ru: C, 52.2; H, 4.62. Found: C, 51.9; H, 4.58. **3g**: IR ν(C=C) 1648 cm⁻¹. Anal. Calcd for C₆₁H₆₉BF₂₄OP₂Ru: C, 50.6; H, 4.77. Found: C, 50.5; H, 4.70. **3h**: IR ν(C=C) 1642 cm⁻¹. Anal. Calcd for C₆₆H₇₁BF₂₄-OP₂Ru: C, 52.5; H, 4.71. Found: C, 52.4; H, 4.79. **3i**: IR ν-(C=C) 1638 cm⁻¹. **3j**: IR: ν(C=C) 1645 cm⁻¹. Anal. Calcd for C₆₄H₇₃BF₂₄OP₂Ru: C, 51.7; H, 4.91. Found: C, 51.5; H, 5.03.

Vinylvinylidene Complexes [Cp*Ru=C=CHCH=CH₂-(PMe^{i}Pr₂)₂][BAr′₄] (4e), [Cp*Ru=C=CHC(CH₃)=CH₂-(PMe^{i}Pr₂)₂][BAr′₄] (4g), [Cp*Ru{=C=CHC=CH(CH₂)₃CH₂}-(PMe^{i}Pr₂)₂][BAr′₄] (4j). A solution of the corresponding 3-hydroxyvinylidene complex was stirred in 5 mL of CH₂Cl₂ at room temperature for 8−10 h. The color changed from yellow-orange to brown. The solvent was evaporated to dryness to give a brown solid. It was washed twice with petroleum ether and dried. Yield: Quantitative. **4e**: IR ν(C=C) 1627 cm⁻¹; ¹H NMR (CDCl₃, 298 K) δ 1.76 s (C₅(CH_3)₅), 4.42, 4.97 (d, $^3J_{H^cH^c}$ = 10.2 Hz, Ru=C=CH^{a}CH^b=CH^c_2), 4.86 (d, $^3J_{H^aH^b}$ = 16.8 Hz, Ru=C=CH^aCH^b=CH$^c_2$), 6.30 (dt, $^3J_{H^bH^a}$ = 16.8 Hz,$^3J_{H^bH^c}$ = 10.2 Hz Ru=C=CH^{a}CH^b=CH$^c_2$); $^{31}P\{^1H\}$ NMR

Table 6. Selected ^{13}C{^{1}H} NMR Data for Hydroxyvinylidene Complexes 3b−j

	R, R′	C$_5$(CH$_3$)$_5$	C$_5$(CH$_3$)$_5$	C$_\alpha$	$^2J_{CP}$	C$_\beta$	C$_\gamma$	R	R′
3b	Ph	10.6	103.3	349.5 t	15.5	115.2		126.5, 128.1, 128.7	
3c	SiMe$_3$	10.3	102.2	345.0 t	15.0	116.3		0.64	
3d	H, H	10.7	103.1	345.4 t	14.7	110.2	53.8		
3e	CH$_3$, H	10.7	103.0	344.1 t	15.5	115.6	61.6	25.3	
3f	Ph, H	10.7	103.2	343.8 t	14.6	114.9	67.5	125.4, 128.4, 128.9	
3g	CH$_3$, CH$_3$	10.7	102.7	344.8 t	14.7	120.9	68.8	33.4	
3h	Ph, CH$_3$	10.6	102.7	344.7 t	14.3	121.2	72.0	123.7, 127.2, 128.4	34.7
3i	Ph, Ph	10.7	102.9	344.3 br		120.7	76.4	125.6, 127.8, 128.4	
3j	C$_5$H$_{10}$	10.7	102.3	345.9 t	16.2	119.6	70.3	22.3, 24.6, 41.1	
3k	H	10.8	103.5	346.5 t	16.0	93.7	-		

^{a} Conditions: 201.2 MHz, CDCl$_3$, 273 K. δ in ppm, and coupling constants in Hz.

(CDCl$_3$, 298 K) δ 37.3 s; ^{13}C{^{1}H} NMR (CDCl$_3$, 298 K) δ 10.5 s (C$_5$(CH$_3$)$_5$), 103.4 s (C$_5$(CH$_3$)$_5$), 110.6 (C$_\beta$), 115.0 (=CH$_2$), 120.9 (C$_\gamma$), 353.9 (t, $^2J_{CP}$ = 15.4 Hz, C$_\alpha$). Anal. Calcd for C$_{60}$H$_{65}$BF$_{24}$P$_2$-Ru: C, 50.9; H, 4.59. Found: C, 51.1; H, 4.66. **4g**: IR ν(C=C) 1625 cm^{-1}; ^{1}H NMR (CDCl$_3$, 298 K) δ 1.70 (s, Ru=C=CHC-(CH$_3$)=CH$_2$), 1.77 s (C$_5$(CH$_3$)$_5$), 4.52 (br, Ru=C=CHC(CH$_3$)=CH$_2$), 4.66, 4.69 (br, Ru=C=CHC(CH$_3$)=CH$_2$); ^{31}P{^{1}H} NMR (CDCl$_3$, 298 K) δ 35.4 s; ^{13}C{^{1}H} NMR (CDCl$_3$, 298 K) δ 10.7 s (C$_5$(CH$_3$)$_5$), 24.0 (Ru=C=CHC(CH$_3$)=CH$_2$), 103.3 s (C$_5$(CH$_3$)$_5$), 112.6 (C$_\beta$), 116.7 (=CH$_2$), 131.8 (C$_\gamma$), 350.4 (t, $^2J_{CP}$ = 15.1 Hz, C$_\alpha$). Anal. Calcd for C$_{61}$H$_{67}$BF$_{24}$P$_2$Ru: C, 51.2; H, 4.69. Found: C, 51.1; H, 4.58. **4j**: IR ν(C=C) 1622 cm^{-1} ^{1}H NMR (CDCl$_3$, 298 K) δ 1.77 s (C$_5$(CH$_3$)$_5$), 1.58, 1.85, 2.13 (m, Ru{=C=CHC⌐=CH(CH$_2$)$_3$CH$_2$}), 4.46 (br, Ru=C=CH), 5.46 (br, Ru{=C=CHC=CH⌐(CH$_2$)$_3$CH$_2$}); ^{31}P{^{1}H} NMR (CDCl$_3$, 298 K) δ 36.0 s; ^{13}C{^{1}H} NMR (CDCl$_3$, 298 K) δ 10.7 s (C$_5$(CH$_3$)$_5$), 21.9, 22.8, 25.6, 30.5 (s, Ru{=C=CHC=CH(CH$_2$)$_3$CH$_2$}), 103.0 s (C$_5$-(CH$_3$)$_5$), 116.8 (C$_\beta$), 124.7 (=CH), 125.4 (C$_\gamma$), 351.4 (t, $^2J_{CP}$ = 15.4 Hz, C$_\alpha$). Anal. Calcd for C$_{64}$H$_{71}$BF$_{24}$P$_2$Ru: C, 52.3; H, 4.83. Found: C, 52.0; H, 4.69.

Allenylidene Complexes [Cp*Ru=C=C=CRR′-(PMe^{i}Pr$_2$)$_2$][BAr′$_4$] (R, R′ = H, Ph (5f), CH$_3$, Ph (5h), Ph, Ph (5i)). The solutions of corresponding 3-hydroxyvinylidene complexes were stirred for 12 h at room temperature in 5 mL of CH$_2$Cl$_2$ and then passed through an acidic alumina column (5 cm height). A brown band was collected in 60−70% yield. The 3-hydroxyalkynyl hydrido complex of diphenylpropargyl alcohol spontaneously dehydrated in the solid state to give the allenylidene complex. **5f**: IR ν(C=C) 1919 cm^{-1}; ^{1}H NMR (CDCl$_3$, 298 K) δ 1.83 s (C$_5$(CH$_3$)$_5$), 7.37, 7.67, 7.79 (Ru=C=C=CHC$_6$H$_5$), 9.39 s (Ru=C=C=CHC$_6$H$_5$); ^{31}P{^{1}H} NMR (CDCl$_3$, 298 K) δ 38.5 s; ^{13}C{^{1}H} NMR (CDCl$_3$, 298 K) δ 10.9 s (C$_5$-(CH$_3$)$_5$), 103.2 s (C$_5$(CH$_3$)$_5$), 142.9 (C$_\gamma$), 129.7, 130.2, 131.7 (Ru=C=C=CHC$_6$H$_5$), 221.9 (C$_\beta$), 301.8 (t, $^2J_{CP}$ = 18.1 Hz, C$_\alpha$). Anal. Calcd for C$_{65}$H$_{67}$BF$_{24}$P$_2$Ru: C, 52.8; H, 4.53. Found: C, 52.7; H, 4.59. **5h**: IR ν(C=C) 1914 cm^{-1}; ^{1}H NMR (CDCl$_3$, 298 K) δ 1.45 s (Ru=C=C=C(CH$_3$)C$_6$H$_5$), 1.84 s (C$_5$(CH$_3$)$_5$), 7.36, 7.65, 7.99 (Ru=C=C=C(CH$_3$)C$_6$H$_5$); ^{31}P{^{1}H} NMR (CDCl$_3$, 298 K) δ 39.3 s; ^{13}C{^{1}H} NMR (CDCl$_3$, 298 K) δ 11.1 s (C$_5$(CH$_3$)$_5$), 102.5 s (C$_5$(CH$_3$)$_5$), 30.7 (Ru=C=C=C(CH$_3$)C$_6$H$_5$), 151.5 (C$_\gamma$), 126.1, 129.5, 131.8 (Ru=C=C=C(CH$_3$)C$_6$H$_5$), 211.1 (C$_\beta$), 295.1 (t, $^2J_{CP}$ = 18.2 Hz, C$_\alpha$). Anal. Calcd for C$_{66}$H$_{69}$BF$_{24}$P$_2$Ru: C, 53.1; H, 4.63. Found: C, 52.8; H, 4.66. **5j**: IR ν(C=C) 1916 cm^{-1}; ^{1}H NMR (CDCl$_3$, 298 K) δ 1.80 s (C$_5$(CH$_3$)$_5$), 7.37, 7.64, 7.92 (Ru=C=C=C(C$_6$H$_5$)$_2$); ^{31}P{^{1}H} NMR (CDCl$_3$, 298 K) δ 39.4 s; ^{13}C{^{1}H} NMR (CDCl$_3$, 298 K) δ 11.0 s (C$_5$(CH$_3$)$_5$), 102.9 s (C$_5$(CH$_3$)$_5$), 153.2 (C$_\gamma$), 125.9, 128.6, 130.6 (Ru=C=C=C(C$_6$H$_5$)$_2$), 217.1 (C$_\beta$), 294.9 (t, $^2J_{CP}$ = 18.7 Hz, C$_\alpha$). Anal. Calcd for C$_{71}$H$_{71}$-BF$_{24}$P$_2$Ru: C, 54.9; H, 4.57. Found: C, 55.0; H, 4.69.

X-ray Structure Determinations. Crystals of **2a**, **2i**, and **3c** were obtained by slow diffusion of petroleum ether into diethyl ether solutions at −20 °C. Crystal data and experimental details are given in Table 1. X-ray data were collected on a Bruker Smart CCD area detector diffractometer (graphite-monochromated Mo Kα radiation, λ = 0.710 73 Å, 0.3° ω-scan frames covering complete spheres of the reciprocal space). Corrections for Lorentz and polarization effects, for crystal decay, and for absorption were applied. All structures were solved by direct methods using the program SHELXS97.[26] Structure refinement on F^2 was carried out with the program SHELXL97.[26] ORTEP[27] was used for plotting.

For the compound **2a** seven of the CF$_3$ groups were split, and the predominantly occupied F sites were refined with anisotropic U_{ij} values, whereas the subordinate F sites were refined with a common isotropic U value for all of them. All other non-hydrogen atoms were anisotropically refined. The hydride H(1Ru) in **2a** was treated with a DFIX restraint.[26] All other hydrogens were refined in idealized positions riding on the atoms to which they were bonded.

For the compound **2i** six of the CF$_3$ groups were split, and the predominantly occupied F sites were refined with aniso-tropic U_{ij} values, whereas the subordinate F sites were refined with a common isotropic U value for all of them. Other non-hydrogen atoms, including those in the solvate molecule Et$_2$O, were anisotropically refined. The hydride atom H(1Ru) was localized and isotropically refined. For all other hydrogen atoms the SHELXL riding model was used.

In the case of compound **3c** relatively high anisotropic thermal displacements were found for the SiMe$_3$ group and seven CF$_3$ groups. Split refinement was checked, yielding significantly lower R values, but a nonsplit model was preferred in this case because of its simplicity. All non-hydrogen atoms were anisotropically refined. Hydrogen atoms were refined in idealized positions riding on the atoms to which they were bonded.

Results and Discussion

The complex [Cp*Ru(PMe^{i}Pr$_2$)$_2$][BAr′$_4$] (**1**) reacts with 1-alkynes HC≡CR at 0 °C in dichloromethane, affording the Ru^{IV} alkynyl hydrido derivatives [Cp*RuH(C≡CR)-(PMe^{i}Pr$_2$)$_2$][BAr′$_4$] (R = COOMe (**2a**), Ph (**2b**), SiMe$_3$ (**2c**)). Likewise, the reaction of **1** with alkynols HC≡CC(OH)RR′ under the same conditions yielded the corresponding hydroxyalkynyl hydrido derivatives [Cp*RuH(C≡CC(OH)RR′)(PMe^{i}Pr$_2$)$_2$][BAr′$_4$] (R, R′ = H, H (**2d**), H, Me (**2e**), H, Ph (**2f**), Me, Me (**2g**), Me, Ph (**2h**), Ph, Ph (**2i**), C$_5$H$_{10}$ (**2j**)). Compounds **2a−j** are off-white or pale yellow materials, which exhibit characteristic ν(C≡C) and ν(RuH) (weak) bands in their IR spectra.

(26) (a) SHELXS97, Program for Crystal Structure Solution; University of Göttingen, 1990. (b) SHELXL97, Program for Crystal Structure Refinement; University of Göttingen, 1997.

(27) (a) Farrugia, L. J. ORTEP-3 for Windows, Version 1.07. *J. Appl. Crystallogr.* **1997**, *30*, 565. (b) Johnson, C. K. ORTEP, A Thermal Ellipsoid Plotting Program; Oak Ridge National Laboratory, Oak Ridge, TN, 1965.
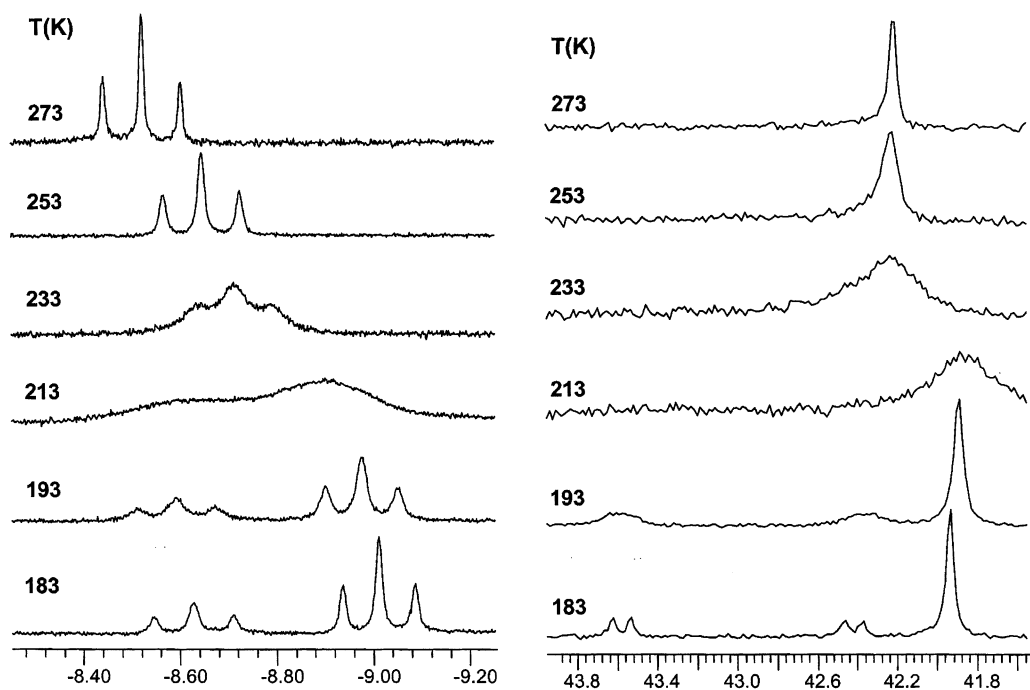
Figure 1. Variable-temperature ^1H (hydride region, left) and $^{31}P\{^1H\}$ (right) NMR spectra of compound **2c** in CD_2Cl_2.

For complexes **2d**−**j**, a weak but sharp band near 3600 cm^{-1} is also present in most cases, attributable to ν-(OH) in the hydroxyalkynyl ligand. With the only exception of compound **2a**, which seems to be remarkably stable, all the other compounds undergo irreversible rearrangement to vinylidene complexes at room temperature in the solid state and in solution. Therefore, they must be stored at −20 °C as solids and handled in solution at 0 °C or below if isomerization is to be avoided. The NMR spectra of these compounds at 0 °C in CD_2Cl_2 (Tables 2 and 3) match in general the pattern previously observed for the complexes [Cp*RuH-(C≡CR)(PP)][BPh$_4$] and [Cp*RuH(C≡CC(OH)RR′)(PP)]-[BPh$_4$] (PP = dippe,[2,6] (PEt$_3$)$_2$[4,5]). Thus, the hydride resonance appears as a high-field triplet, whereas one singlet is observed in the $^{31}P\{^1H\}$ NMR in most cases, except for **2h**. In this case, the $^{31}P\{^1H\}$ NMR spectrum consists of two overlapping doublets from an AB spin system, resulting from the magnetic nonequivalence of the phosphorus atoms due to the presence of the asymmetric γ-carbon in the alkynyl group, as has been previously noted for other hydroxyalkynyl hydrido complexes.[4−6,8] This should be also the expected $^{31}P\{^1H\}$ NMR pattern for **2e**,**f**, since these compounds also bear an asymmetric γ-carbon in the alkynyl group, but one singlet is observed instead. We have reported that the $^{31}P\{^1H\}$ NMR of [Cp*RuH(C≡CC(OH)HPh)(dippe)]-[BPh$_4$] is temperature dependent, and whereas an AB double doublet is observed at low temperatures, these resonances coalesce into one singlet at +15 °C.[6] This has been interpreted in terms of an averaging of the anisotropy of the phosphorus atom environments through rapid rotation of the CH(OH)Ph group about the C≡C bond, leading to the accidental coincidence of the chemical shifts of the two phosphorus atoms, which remain magnetically inequivalent. This explanation holds also for **2e**,**f**.

   We were interested in detecting possible intermediate species in the course of the formation of the alkynyl

hydrido complexes, i.e., η^2-CH agostic alkyne species. Thus, we monitored by NMR spectroscopy the reactions of the 16-electron complexes [Cp*Ru(PP)][BAr′$_4$] (PP = dippe, (PMe^{i}Pr$_2$)$_2$) with different alkynes in CD_2Cl_2 at 183 K. At this temperature, the ^1H and $^{31}P\{^1H\}$ NMR spectra of the reaction mixture of [Cp*Ru(dippe)][BAr′$_4$] with HC≡CR (R = COOMe, Ph, SiMe$_3$) revealed exclusively the formation of the corresponding alkynyl hydrido derivatives [Cp*RuH(C≡CR)(dippe)][BAr′$_4$] at the expense of [Cp*Ru(dippe)][BAr′$_4$], and no other intermediates were detected. In the case of the reaction of **1** with HC≡CR (R = COOMe, Ph, SiMe$_3$) at 183 K, the ^1H NMR spectra showed two distinct triplet hydride signals, in an approximately 1:2 ratio. The $^{31}P\{^1H\}$ NMR spectra consisted of one relatively sharp resonance for the major component of the mixture and two doublets from an AM spin system (unresolved in the case of the HC≡CCOOMe reaction) for the minor component. When the temperature was raised, the two triplet hydride resonances in the ^1H NMR spectra coalesce into a broad signal, which resolved into one triplet at 233 K. In a similar fashion, the different signals in the $^{31}P\{^1H\}$ spectra coalesce into one broad feature, which sharpens as the temperature is raised. At 273 K, the ^1H and $^{31}P\{^1H\}$ NMR spectra of the in situ reaction of **1** with HC≡CR matched exactly those of **2a**−**c**, respectively. In fact, when the spectra of these compounds were recorded at 183 K, decoalescence to two triplets was observed for the hydride signals in the ^1H spectra and to one singlet plus two doublets in the ^{31}P-$\{^1H\}$ spectra, as shown in Figure 1 for compound **2b**, the original spectra being restored when the temperature is raised again. Thus, as happens in the case of the reaction of [Cp*Ru(dippe)][BAr′$_4$] with 1-alkynes, no intermediates are detected, and the actual species observed are the alkynyl hydrido complexes **2a**−**c**. However, this experiment has exposed an unusual dynamic behavior for the alkynyl hydrido derivatives generated by reaction of **1** with 1-alkynes, which has
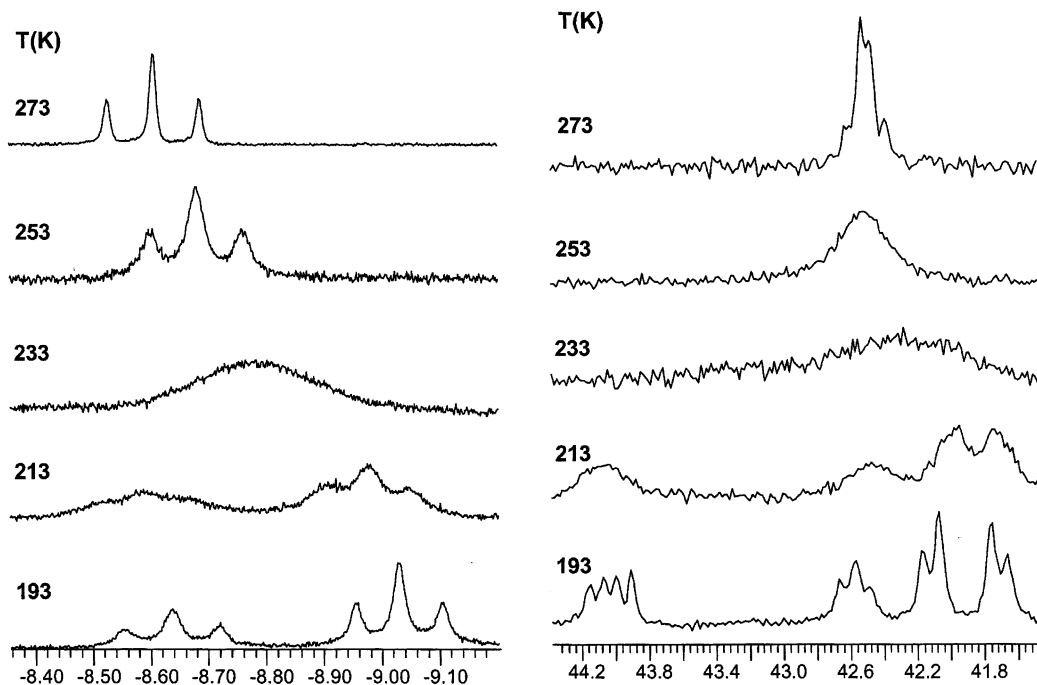
Figure 2. Variable-temperature ^{1}H (hydride region, left) and ^{31}P{^{1}H} (right) NMR spectra of compound **2h** in CD$_2$Cl$_2$.

not been observed for other alkynyl hydrido complexes such as [Cp*RuH(C≡CR)(dippe)]$^+$ [2,6] and [Cp*RuH(C≡CR)(PEt$_3$)$_2$]$^+$.[4,5] This prompted us to undertake detailed variable-temperature NMR studies of compounds **2a**–**j**, to clarify the nature of the species observed at low temperature. Selected ^{1}H and ^{31}P{^{1}H} NMR data at 183 K are also included in Table 2. The ^{1}H NMR spectra of complexes **2a**–**i** all exhibit similar behavior, namely decoalescence of the hydride resonance to two triplet resonances when the temperature is lowered, corresponding to two different alkynyl hydrido isomers which coexist in equilibrium. The ^{31}P{^{1}H} NMR spectra of complexes **2a**–**d,g,i** also show a parallel behavior and are consistent with the presence of two isomers, one with equivalent phosphorus atoms (isomer A) and another with inequivalent phosphorus atoms (isomer B), giving rise to the two doublets (AM spin system). In those cases in which a stereocenter is present at the *γ*-carbon (compounds **2e,f,h**), the ^{31}P{^{1}H} NMR spectra are more complicated, as shown in Figure 2 for compound **2h**, for instance. Three different diastereoisomers are observed at low temperature in these cases. For isomer A, the phosphorus atoms are now inequivalent as well, due to the presence of the stereocenter, and an AB quartet is observed instead of one singlet. The combination of the inequivalent phosphorus atoms of isomer B with the two possible enantiomers of the hydroxyalkynyl ligand gives rise to two different diastereoisomers (B$_1$ and B$_2$), each of them showing two doublets in the ^{31}P{^{1}H} NMR spectra (two AM spin systems). The fact that triplet resonances are observed in all cases for the hydride protons of the possible isomers, even for those with inequivalent phosphorus atoms, indicates that the coupling constants $^2J_{HP}$ and $^2J_{HP'}$ in each case must have very similar values, as has been found in systems such as [CpRuH(PMe^{i}Pr$_2$)(PPh$_3$)] and [CpRuH$_2$(PMe^{i}Pr$_2$)(PPh$_3$)]-[BPh$_4$].[21] The variable-temperature ^{1}H and ^{31}P{^{1}H} NMR spectra of compound **2j** (Figure 3) show a slightly different behavior. At

variance with the ^{1}H NMR spectra of compounds **2a**–**i**, which exhibit two triplet hydride resonances when the temperature is lowered, in the case of **2j** four overlapping triplet signals appear. Despite the fact that **2j** bears no chiral center, its variable-temperature ^{31}P{^{1}H} spectra are very complicated, behaving as if indeed a stereogenic group were present.

Several possible interpretations can be provided in order to explain the unprecedented dynamic behavior of compounds **2a**–**j**. We have observed very recently a similar pattern for the variable-temperature NMR spectra of the dihydride complex [Cp*RuH$_2$(PPh^{i}Pr$_2$)$_2$]-[BAr′$_4$].[22b] These features have been rationalized by assuming an equilibrium between rotamers of the phosphine in the transoid dihydride. For each rotational isomer, one group on each phosphine is pointing away from Cp*, and the other two are to the sides; hence, several possible rotamers are possible. If this is also the case for compounds **2a**–**j**, the species involved should be all transoid alkynyl hydrides, differing in the relative orientation of the methyl and isopropyl substituents around the Ru−P bonds, as shown in Scheme 1. Thus, A and B should be then more properly referred to as rotamers or rotameric isomers. Scheme 2 shows the diastereomeric species, which would result from the occurrence of rotamers in combination with the presence of one chiral center at the *γ*-carbon atom (compounds **2e,f,h**). In case of rotamer A, two enantiomers are possible, depending on the configuration of the stereogenic *γ*-carbon, but these are not distinguishable by NMR spectroscopy. At variance with this, for rotamer B two diastereoisomers, namely B$_1$ and B$_2$, result from the different configurations of the asymmetric *γ*-carbon, and as such they give separate resonances in the ^{31}P-{^{1}H} NMR spectra. However, the chemical shift for the hydride resonances of B$_1$ and B$_2$ must coincide, since only one signal is observed for these isomeric species in their ^{1}H NMR spectra. The situation of compound **2j** is unique. At 183 K, four hydridic protons appear in the
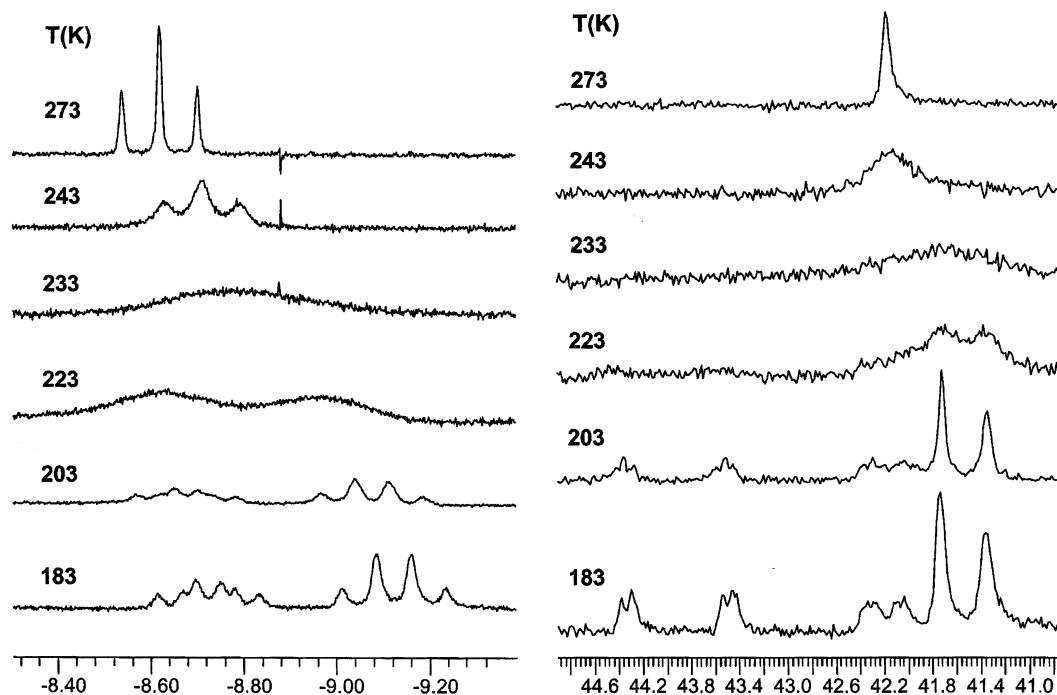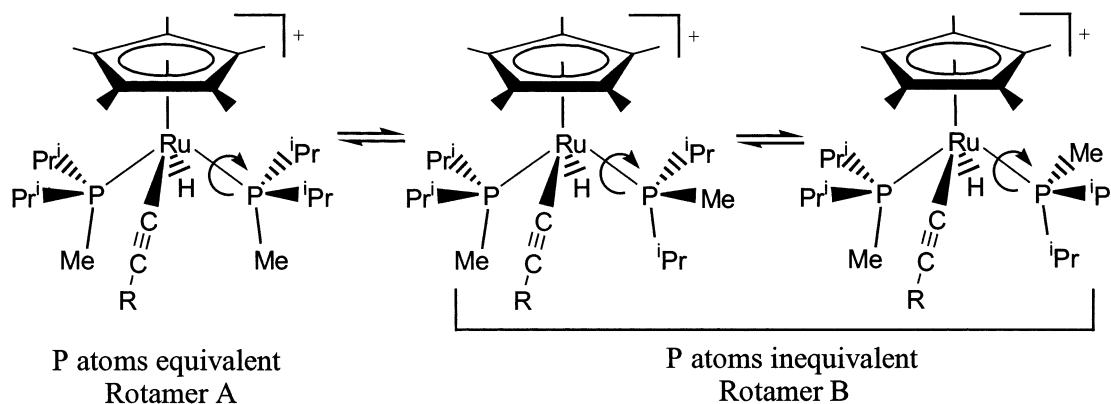
Figure 3. Variable-temperature ^{1}H (hydride region, left) and ^{31}P{^{1}H} (right) NMR spectra of compound **2j** in CD$_2$Cl$_2$.

Scheme 1.   Equilibrium between Rotameric Isomers of Alkynyl Hydrido Complexes
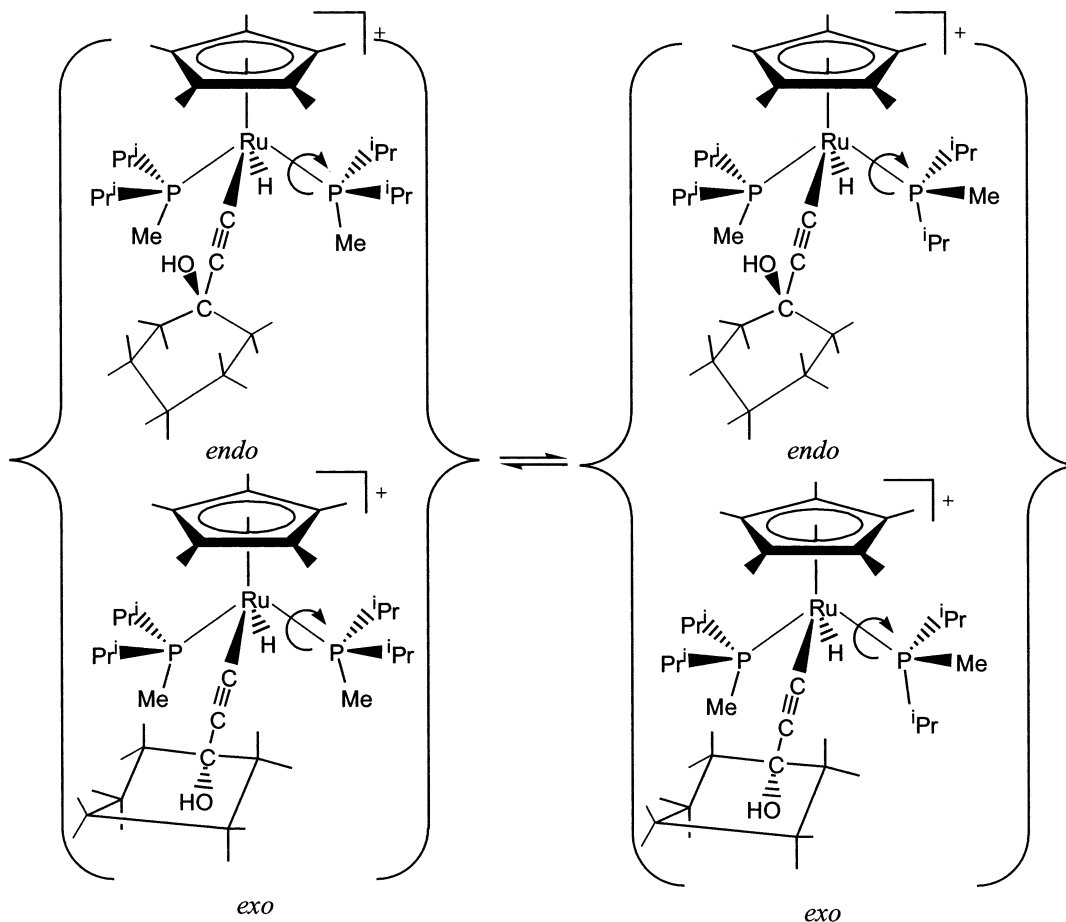

P atoms equivalent
Rotamer A

P atoms inequivalent
Rotamer B

^{1}H NMR spectrum, and signals attributable to four different species are present in the ^{31}P{^{1}H} NMR spectrum: two singlets and two AM sets of two doublets each (Figure 3 and Table 2). In this particular case, the possible conformations of the cyclohexyl ring might be playing an important stereochemical role. We have rationalized this in terms of two possible orientations of the cyclohexyl ring relative to the OH group, namely exo and endo, for each of the situations A and B, giving rise to a total of four possible stereoisomers, A$_1$/A$_2$ and B$_1$/B$_2$, as shown in Scheme 3. Alternatively, isomers could also arise from the occupation of the OH in axial and equatorial positions of the cyclohexyl ring, rather than exo/endo orientations.

Although the assumption of the equilibrium between phosphine rotamers seems to justify the observed variable-temperature NMR spectra, an alternative explanation can be proposed on the basis of the hypothesis of stereochemical nonrigidity for the half-sandwich alkynyl hydrido cations. It must be noted that these complexes are formally seven-coordinate and that the lack of stereochemical rigidity is a typical feature of such species.[28] An interesting possibility is therefore to
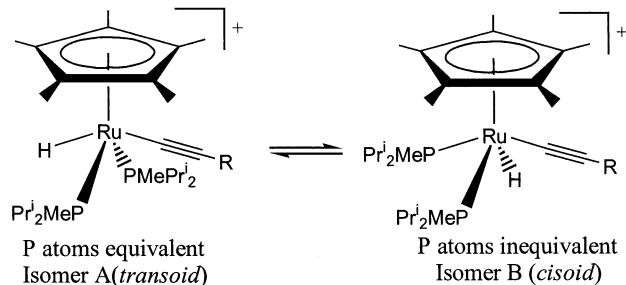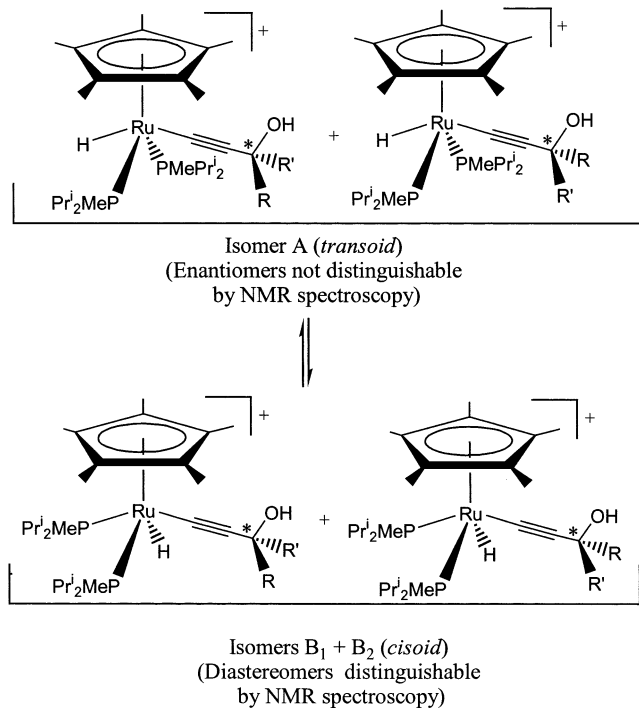
consider an equilibrium between transoid (isomer A) and cisoid (isomer B) stereoisomers of complexes **2d–j**, as shown in Scheme 4. Since the cisoid isomers always have inequivalent phosphorus atoms, these always appear as two doublets in their ^{31}P{^{1}H} NMR spectra. The presence of one triplet for the hydride ligand in these isomers should be again attributed to the accidental coincidence of the values of $^2J_{HP}$ and $^2J_{HP'}$. Scheme 5 displays the equilibrium between the A and B types of stereoisomers in the case of hydroxyalkynyl hydrido complexes bearing an asymmetric γ-carbon. The pair of enantiomers of the transoid isomer (A$_1$/A$_2$) is not distinguishable by NMR spectroscopy, giving rise to one single resonance in their NMR spectra, whereas in case of the cisoid isomer, the possible configurations of the asymmetric γ-carbon lead to two different diastereoisomers, B$_1$ and B$_2$. The particular case of compound **2j** can be also consistently explained by considering a transoid/cisoid equilibrium in combination with the possible exo/endo orientations of the OH group, as shown in Scheme 6.

(28) Drew, M. G. B., *Prog. Inorg. Chem.* **1977**, *23*, 67.

Scheme 2. Equilibrium between Rotameric Isomers of Hydroxyalkynyl Hydrido Complexes Bearing a Chiral γ-Carbon

Rotamer A
(Enantiomers not distinguishable
by NMR spectroscopy)

Rotamers B₁ + B₂
(Diastereomers distinguishable
by NMR spectroscopy)
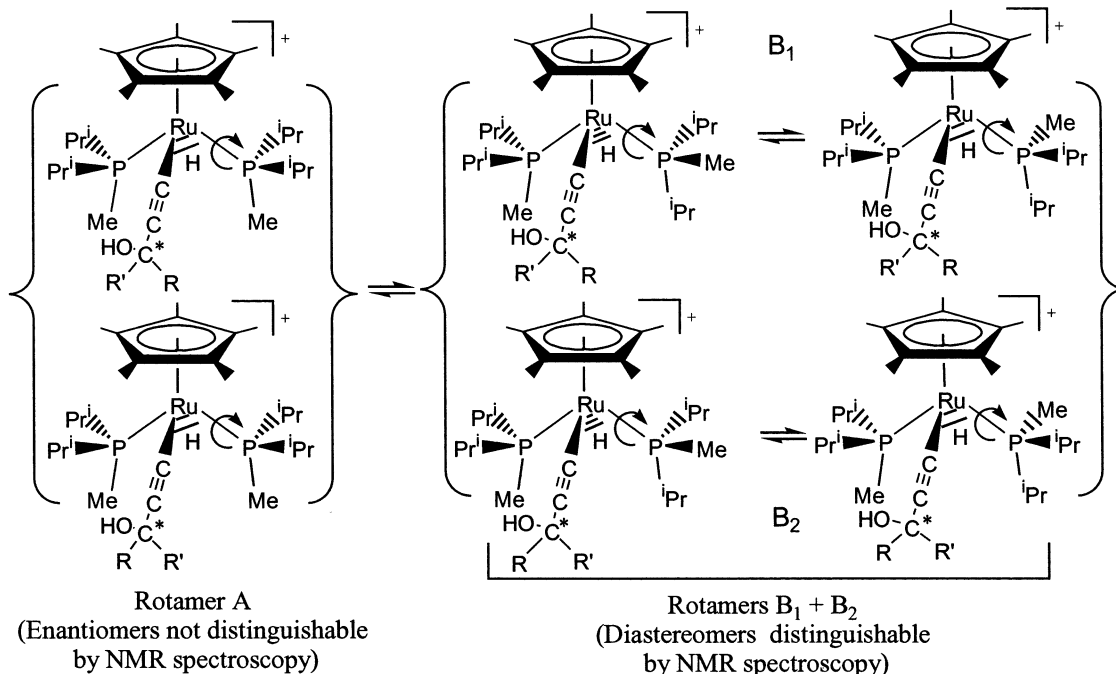
Scheme 3. Equilibrium between Rotameric and Exo/Endo Isomers of Compound 2j

endo

endo

exo

exo

In summation, the occurrence of rotameric isomers and a possible transoid/cisoid equilibrium are both reasonable proposals that justify the observed dynamic behavior of complexes **2a–j**. The latter is particularly attractive, in connection with the activation of C−H

bonds and the postulated existence of species containing a η^2-HC≡CR ligand.[12−14] We have performed a dynamic NMR line shape fitting simulation on the ¹H variable-temperature NMR spectra of complexes **2a–j**. This has led to the determination of thermodynamic and activa-

Scheme 4. Equilibrium between Transoid and Cisoid Isomers of Alkynyl Hydrido Complexes

P atoms equivalent
Isomer A(*transoid*)

P atoms inequivalent
Isomer B (*cisoid*)

Scheme 5. Equilibrium between Transoid and Cisoid Isomers of Hydroxyalkynyl Hydrido Complexes Bearing an Asymmetric γ-Carbon

Isomer A (*transoid*)
(Enantiomers not distinguishable
by NMR spectroscopy)

Isomers B$_1$ + B$_2$ (*cisoid*)
(Diastereomers distinguishable
by NMR spectroscopy)

Figure 4. ORTEP drawing (30% thermal ellipsoids) of the cation [Cp*RuH(C≡CCOOMe)(PMe^{i}Pr$_2$)$_2$]$^+$ in complex **2a**. Hydrogen atoms, except hydride, have been omitted. Selected bond lengths (Å) and angles (deg) with estimated standard deviations in parentheses: Ru−C(1), 2.264(4); Ru−C(2), 2.256(4); Ru−C(3), 2.235(2); Ru−C(4), 2.268(4); Ru−C(5), 2.318(5); Ru−P(1), 2.368(1); Ru−P(2), 2.389(1); Ru−C(31), 2.006(4); C(31)−C(32), 1.202(5); C(32)−C(33), 1.431(6); C(33)−O(1), 1.186(5); C(33)−O(2), 1.315(5); H(1Ru)−Ru−C(31), 132; P(1)−Ru−P(2), 106.29(4); Ru−C(31)−C(32), 177.8(4); C(31)−C(32)−C(33), 175.2(5); O(1)−C(33)−O(2), 122.9(4).

tion parameters listed in Table 4 for the equilibrium between A-type and B-type isomers. With the only exception of compound **2i**, isomer A predominates over B at low temperature in all cases, as indicated by the values of K_{eq} being less than 1. ΔG^{298} has in all cases a value very close to 0 kcal mol^{-1}, suggesting that the energy difference between the A and B isomers is indeed very small. The activation energy $\Delta G^{\ddagger 298}$ is close to 11 kcal mol^{-1} for all compounds, and it is worth mentioning that the negative values of $\Delta S^{\ddagger}$ EW consistent with an "ordered" transition state in the pathway from isomer A to isomer B. Changing hydride to deuteride apparently does not affect the thermodynamic and activation parameters. This is supported by the observation that the variation with temperature of the ^{31}P{^{1}H} NMR spectra of the deuterated derivative [Cp*RuD(C≡CPh)(PMe^{i}Pr$_2$)$_2$][BAr′$_4$] (**2b−d**) is identical with that of the nondeuterated complex **2b**. Given the fact that compound **2a** is stable at room temperature both in the solid state and in solution and that it does not rearrange to its vinylidene tautomer, its X-ray crystal structure was determined. An ORTEP view of the complex cation is shown in Figure 4. The cation has a four-legged piano-
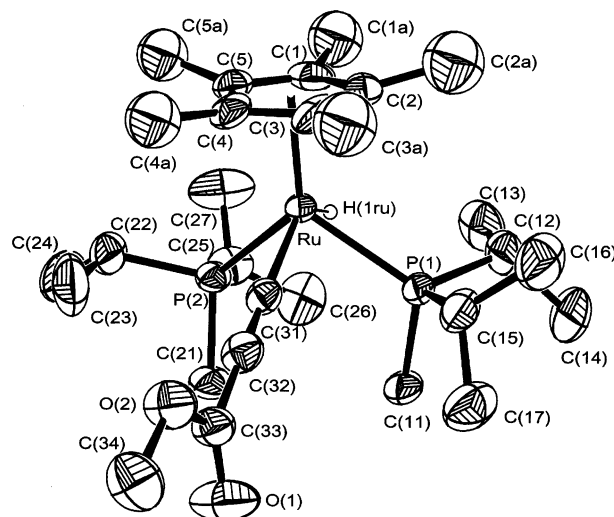
stool structure with a transoid disposition of hydride and alkynyl ligands, very similar to that observed for the complex [Cp*RuH(C≡CCOOMe)(dippe)][BPh$_4$].[2] The dimensions of the alkynyl ligand compare well with data in the literature.[2,3,5,8,9,29] The methyl substituents of the PMe^{i}Pr$_2$ ligands point away from Cp* and the ^{i}Pr groups to the sides. The torsion angle C(11)−P(1)−P(2)−C(21) has a value of 21.4°, which corresponds to a slightly staggered disposition of the phosphine substituents relative to each other. Therefore, it seems confirmed that the structure in the solid state for **2a** corresponds to the transoid isomer. We were most interested in the solid-state structure for compound **2i**, which has the equilibrium shifted in solution toward the B-type isomer. However, this compound readily isomerizes to its hydroxyvinylidene tautomer at room temperature both in solution and in the solid state (vide infra). We managed to grow crystals of **2i** at low temperature, and once isolated, they were immediately subjected to low-temperature X-ray structure analysis in order to avoid tautomerization. The complex crystallized as the diethyl ether solvate. An ORTEP view of the structure of the complex cation is shown in Figure 5. Again, the cation has a four-legged piano-stool structure, with a transoid disposition of hydride and alkynyl ligands: i.e., the same as in **2a** or in [Cp*RuH(C≡CCOOMe)(dippe)][BPh$_4$].[2] The OH group of the hydroxyalkynyl ligand is clearly hydrogen-bonded to the oxygen atom of the diethyl ether solvate molecule, with a bond distance O(1)···O(2s) of 2.824(4) Å (calculated H(1OH)···O(2s) = 2.031 Å). In this case, the disposition of the substituents around the phosphorus atoms, as well as the relative orientation

(29) (a) Bianchini, C.; Frediani, P.; Masi, D.; Peruzzini, M.; Zanobini, F. *Organometallics* **1994**, *13*, 4616. (b) Jiménez-Tenorio, M.; Puerta, M. C.; Valerga, P. *J. Chem. Soc., Chem. Commun.* **1993**, 1750.
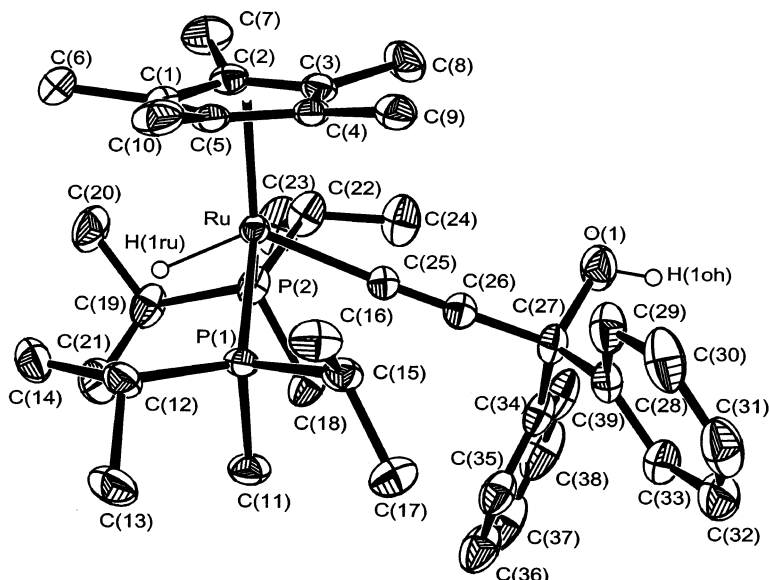
Figure 5. ORTEP drawing (30% thermal ellipsoids) of the cation of [Cp*RuH(C≡CC(OH)Ph$_2$)(PMe^{i}Pr$_2$)$_2$]$^+$ in complex **2i**. Hydrogen atoms, except hydride and OH, have been omitted. Selected bond lengths (Å) and angles (deg) with estimated standard deviations in parentheses: Ru−H(1Ru), 1.51(3); Ru−C(1), 2.284(3); Ru−C(2), 2.324(3); Ru−C(3), 2.261(3); Ru−C(4), 2.238(2); Ru−C(5), 2.274(3); Ru−P(1), 2.3589(8); Ru−P(2), 2.3842(9); Ru−C(25), 2.031(3); C(25)−C(26), 1.203(4); C(26)−C(27), 1.487(4); C(27)−O(1), 1.432(4); C(27)−C(34), 1.536(4); C(27)−C(28), 1.538(4); O(1)−H(1OH), 0.83; H(1Ru)−Ru−C(25), 133(1); P(1)−Ru−P(2), 106.11(3); Ru−C(25)−C(26), 176.5(2); C(25)−C(26)−C(27), 173.4(3); C(26)−C(27)−O(1), 105.6(2); C(26)−C(27)−C(28), 111.9(2); C(26)−C(27)−C(34), 105.8(2).

Scheme 6. Equilibrium between Transoid/Cisoid and Exo/Endo Isomers of Compound 2j

transoid (A$_1$ + A$_2$)   *cisoid* (B$_1$ + B$_2$)
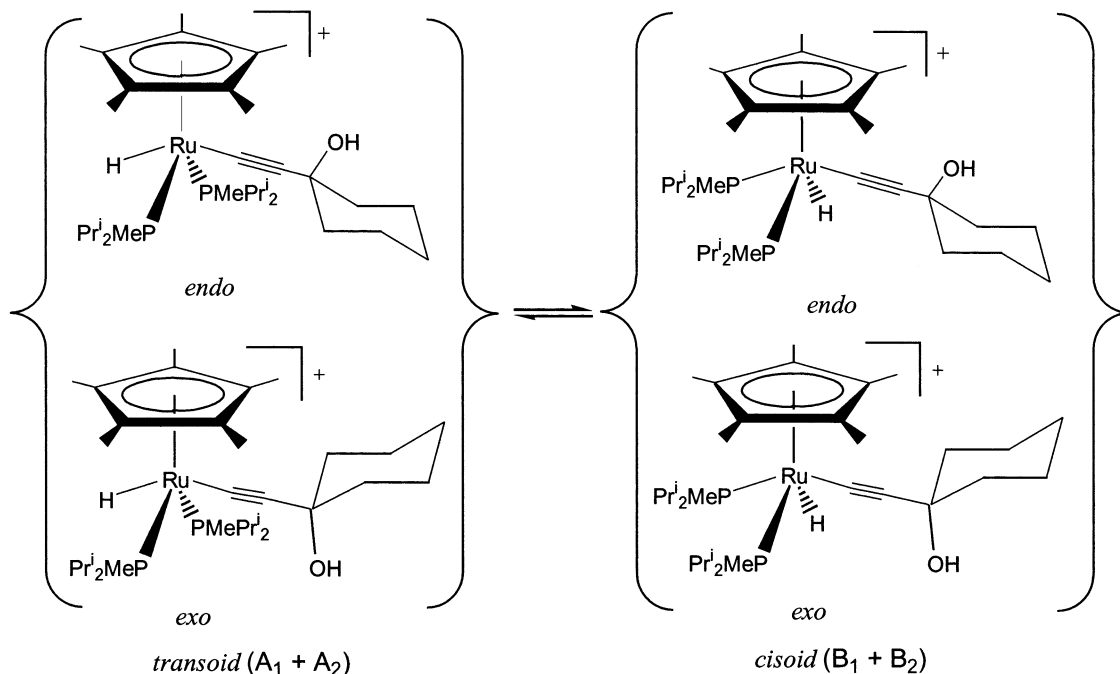
of the phosphine groups, is very similar to that found in **2a** (torsion angle C(11)−P(1)−P(2)−C(18) = 24.6°). Thus, also in this case we find the transoid structure to be the most stable isomer in the solid state.

Having reached this point and taking into consideration all data obtained, we are still not completely certain of the nature of the species involved in the fluxional process which affects compounds **2a**−**j**, since both of the alternatives presented are consistent with experimental observations. Although the X-ray crystal structures have shown only transoid cations, we must note the small differences in energy between the A and

B isomers, which can be easily overcome by the packing forces in the crystal, leading to only one of the isomers, namely transoid, to be present. An intramolecular transoid/cisoid rearrangement does not involve Ru−H cleavage, and therefore, we should not expect a great change in the activation parameters of the deuterated isotopomer. Furthermore, no isotopic effect has been observed for the tautomerization of [Cp*RuH(C≡CPh)(dippe)]$^+$ to [Cp*Ru=C=CHPh(dippe)]$^+$ in solution, even when this process occurs through a dissociative pathway.[2] On the other hand, the observed dynamic behavior has only one recent precedent in the case of

Scheme 7
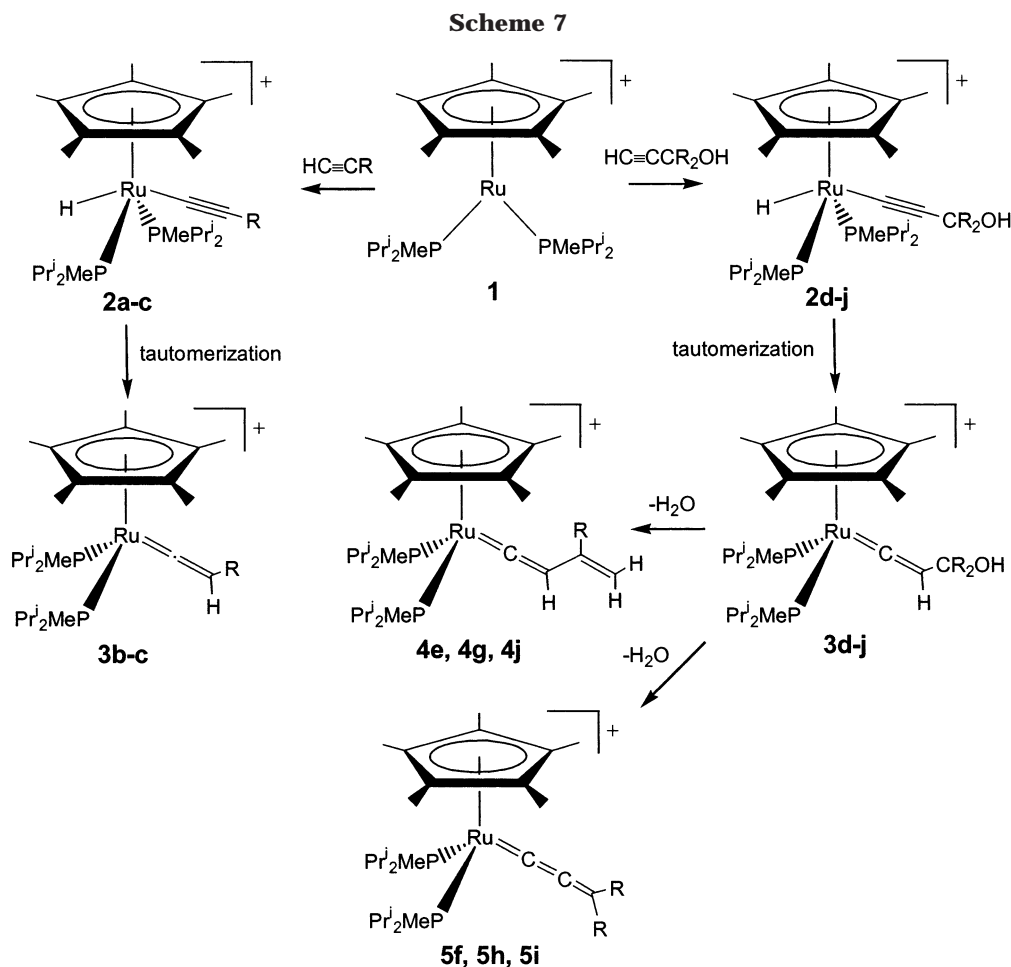
[Cp*RuH$_2$(PPh^{i}Pr$_2$)$_2$][BAr′$_4$].[22b] If we accept as valid the proposal that invokes phosphine rotamers, we should expect that this sort of dynamic behavior would have been observed more often, in other circumstances. For instance, we have observed decoalescence of the ^{31}P{^{1}H} NMR resonances in the case of the complexes [TpRuCl-(PMe^{i}Pr$_2$)$_2$][30] and [Cp*RuCl(PMe^{i}Pr$_2$)$_2$].[21] However, in these cases, one single resonance gave rise to a partially resolved AB pattern, rather than to an equilibrium mixture of isomers. It should have been expected to observe a similar fluxional behavior in other related compounds such as [Cp*RuH$_2$(PMe^{i}Pr$_2$)$_2$][BPh$_4$][21] or the vinylidene derivatives **2b−j** (vide infra), but this was not the case. Since this dynamic behavior is rather exceptional, we are inclined to suggest that the process responsible for it is actually the rapid equilibrium between fluxional transoid and cisoid isomers of compounds **2a−j**. It is likely that the backbone carbon chain in the dippe ligand prevents this process from occuring to any appreciable extent in the [Cp*RuH(C≡CR)-(dippe)][BPh$_4$][2,6] complexes, whereas for [Cp*RuH(C≡CR)(PEt$_3$)$_2$][BPh$_4$][4,5] derivatives, the activation energy could be lower than with PMe^{i}Pr$_2$ as coligand, and hence the slow exchange limit is not reached within the temperature range in which the NMR spectra are measured. However, given the fact that there is no rotation around the Ru−P bond in [Cp*RuH(C≡CR)-(dippe)]$^+$ and that the possible rotamers of [Cp*RuH-

(C≡CR)(PEt$_3$)$_2$]$^+$ would be identical, the proposal that invokes hindered rotation around the Ru−P bond cannot be ruled out in any case.

Vinylidene and Allenylidene Complexes. With the only exception of compound **2a**, all the other alkynyl and hydroxyalkynyl hydrido complexes **2b−j** spontaneously rearrange to their vinylidene or 3-hydroxyvinylidene isomers, both in solution and in the solid state (Scheme 7). In fact, the most efficient procedure for the preparation of the vinylidene and hydroxyvinylidene complexes **3b−j** was the heating of solid samples of the corresponding alkynyl hydrido derivative **2b−j** at 30 °C for over a period of 3−6 h. The process can be monitored by IR spectroscopy, following the dissappearance of the ν(C≡C) band near 2100 cm^{-1} and the concomitant increase in the ν(C=C) band of the vinylidene ligand in the range 1620−1640 cm^{-1}. The spectral properties of the vinylidene and hydroxyvinylidene complexes **3b−j** (Tables 5 and 6) are consistent with data reported in the literature for related complexes.[3−6,13] The X-ray crystal structure of **3c** was determined. An ORTEP view of the complex cation is shown in Figure 6. The complex has a three-legged piano-stool structure, with Ru−C(31) and C(31)−C(32) separations similar to those found in other vinylidene complexes.[2,5,13,31] The dihedral angle Si−C(32)−Ru−centroid has a value of 84.2°, very close to perpendicularity, whereas the torsion angle C(21)−P(2)−P(1)−C(11) is 68.6°, indicative of a completely

(30) Jiménez-Tenorio, M. A.; Jiménez-Tenorio, M.; Puerta, M. C.; Valerga, P. *J. Chem. Soc., Dalton Trans.* **1998**, 3601.

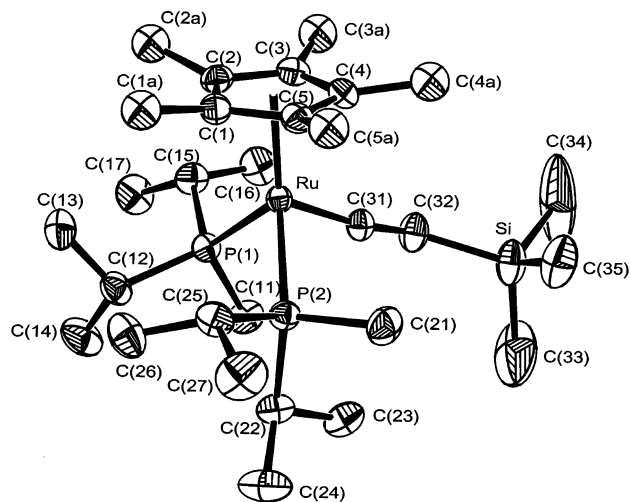(31) Jiménez-Tenorio, M. A.; Jiménez-Tenorio, M.; Puerta, M. C.; Valerga, P. *Organometallics* **2000**, *19*, 1333.

Figure 6. ORTEP drawing (30% thermal ellipsoids) of the cation of $[Cp*Ru=C=CHSiMe_3(PMe^iPr_2)_2][BAr'_4]$ in complex **3c**. Hydrogen atoms have been omitted. Selected bond lengths (Å) and angles (deg) with estimated standard deviations in parentheses: Ru−C(1), 2.345(3); Ru−C(2), 2.366(3); Ru−C(3), 2.294(3); Ru−C(4), 2.259(3); Ru−C(5), 2.289(3); Ru−P(1), 2.3701(8); Ru−P(2), 2.3621(9); Ru−C(31), 1.850(3); C(31)−C(32), 1.289(5); C(32)−Si, 1.876(5); Si−C(33), 1.856(9); Si−C(34), 1.797(8); Si−C(35), 1.842(6); P(1)−Ru−P(2), 96.08(3); P(1)−Ru−C(31), 87.75(9); P(2)−Ru−C(31), 93.5(1); Ru−C(31)−C(32), 171.6(3); C(31)−C(32)−Si, 136.3(3).

staggered conformation of the methyl substituents in the PMe^iPr_2 ligands. The relative orientation of the substituents of the PMe^iPr_2 groups in the solid state makes the phosphorus atoms nonequivalent, unless we assume fast spinning around the Ru−P bonds. However, as has been already mentioned above, no decoalescence was observed in the low-temperature $^{31}P\{^1H\}$ NMR spectrum of **3c** or in the $^{31}P\{^1H\}$ NMR spectra of any other vinylidene or hydroxyvinylidene complex **3b−j**. Although this observation seems to support the idea that the fluxional behavior exhibited by compounds **2a−j** might be attributable to a transoid/cisoid equilibrium rather than to an equilibrium between phosphine rotamers, it must be noted that the angles C(31)−Ru−P(1) and C(31)−Ru−P(2) in **3c** are ca. 10° greater than the corresponding angles in complexes **2a,i**. Therefore, a less hindered rotation around the Ru−P bond is expected for **3c**, meaning a lower barrier to rotation and, hence, a lower coalescence temperature.

All hydroxyvinylidene complexes, with the only exception of **3d**, undergo dehydration leading to either vinylvinylidene complexes (**4e,g,j**) or allenylidene complexes (**5f,h,i**) (Scheme 7). The dehydration is accomplished by stirring a dichloromethane solution of the corresponding hydroxyvinylidene complex at room temperature for 8−10 h. In case of allenylidene complexes, after 12 h of stirring, the solution was passed through a column of acidic alumina, affording the pure dehy-

drated product.[5,32] Compound **3i** also dehydrates spontaneously in the solid state to give the allenylidene complex **5i**. The spectral properties of these vinylvinylidene and allenylidene complexes are consistent with their formulation and compare well with our data for other related $[Cp*Ru=C=CHC(R)=CH_2(P_2)][BPh_4]$ and $[Cp*Ru=C=C=CR_2(P_2)][BPh_4]$ systems (P_2 = dippe,[3,6] $(PEt_3)_2$[4,5]). The observed pattern of dehydration of the hydroxyvinylidene complexes follows in general the pathways reported in previous works[4−6] and do not require further comment.

Conclusions

The reaction of the 16-electron complex $[Cp*Ru(PMe^iPr_2)_2][BAr'_4]$ with 1-alkynes or 3-hydroxyalkynes leads to the corresponding alkynyl hydrido or hydroxyalkynyl hydrido complexes. These complexes have four-legged piano-stool structures, as shown by X-ray structure analysis, and display a fluxional behavior in solution which has been explained in terms of two mechanistic proposals: (a) hindered rotation around the Ru−PMe^iPr_2 bond and (b) rapid equilibration between transoid and cisoid stereoisomers. Dynamic NMR line shape analysis revealed a very small energy difference between the two stereoisomers in equilibrium (less than 1 kcal mol^{-1}) and an activation energy of 11 kcal mol^{-1} at 298 K for the process. Proposals a and b both satisfactorily explain the observed dynamic behavior, and neither of them can be disregarded in principle. However, the failure to observe such behavior in other related compounds which give rise to rotamers seems to be more consistent with the equilibrium between cisoid and transoid stereoisomers (proposal b). In any case, further evidence is necessary to prove this unambiguously. Isomerization to vinylidene tautomers takes place smoothly in most cases, both in solution and in the solid state. Hydroxyvinylidene complexes undergo further dehydration reactions, leading to either vinylvinylidene complexes or allenylidene complexes, depending on the substituents present on the hydroxyvinylidene ligand.

Supporting Information Available: Tables of X-ray structural data, including data collection parameters, positional and thermal parameters, and bond distances and angles for complexes **2a,i** and **3c**. This material is available free of charge via the Internet at http://pubs.acs.org.

OM020940N

(32) (a) Martin, M.; Werner, H. *J. Chem. Soc., Dalton Trans.* **1996**, 2275. (b) Werner, H.; Rappert, T.; Wiedemann, R.; Wolf, J.; Mahr, N. *Organometallics* **1994**, *13*, 2721. (c) Werner, H.; Lass, R. W.; Gevert, O.; Wolf, J. *Organometallics* **1997**, *166*, 4077.